Metastable conduction states in Mo_2S_3: Conductivity fluctuations

R. L. Fagerquist,* Roger D. Kirby, and Edgar A. Pearlstein
Behlen Laboratory of Physics, University of Nebraska–Lincoln, Lincoln, Nebraska 68588-0111
(Received 14 September 1988)

In this paper, we present the results of measurements of the frequency and temperature dependences of the electrical noise in Mo_2S_3. It will be seen that the frequency dependence of the noise is completely consistent with the double-well potential model for the carriers in Mo_2S_3 introduced in an earlier paper [Phys. Rev. B **38**, 3973 (1988)]. In the earlier paper, we showed that at temperatures below 145 K, the carriers in Mo_2S_3 could exist in either a weakly conducting ground state or a relatively highly conducting metastable state. The conductivity behavior of Mo_2S_3 was found to be consistent with a phenomenological double-well potential model in which the ground state is separated from the metastable state by a large energy barrier of height W. The model predicts that carriers transfer from one state to the other by thermal activation, so that the lifetime of the carriers in the metastable state varies strongly with temperature according to $\tau=\tau_0\exp(W/kT)$, with $W=0.25$ eV and $\tau_0=5\times10^{-15}$ sec. The magnitude of the electrical noise measurements reported here, when coupled with the magnitude of the conductivity and the carrier density, require either that the carriers in Mo_2S_3 have a very large mobility ($\sim4\times10^4$ cm^2/V s), or that the carriers behave cooperatively, as they would if Mo_2S_3 were a charge-density-wave system.

I. INTRODUCTION

Mo_2S_3 is a quasi-one-dimensional compound in which single crystals grow as long fibers parallel to the crystalline b axis. The average room-temperature structure is monoclinic, with inequivalent zig-zag chains of Mo atoms parallel to the b axis. Electrical resistance,[1–5] thermoelectric power,[1,5] x-ray diffraction,[1,6–8] magnetic susceptibility,[1,3] and internal friction measurements[9] show that Mo_2S_3 undergoes at least two phase transitions below room temperature. The resistance and susceptibility measurements of Rashid *et al.*[3] show phase transitions involving a loss of Fermi surface at 182 and 145 K on cooling, with both phase transitions having considerable hysteresis. The 145-K phase transition seems to be quite sluggish.[3–5] X-ray diffraction measurements by Deblieck *et al.*[8] show that the 182-K phase transition on cooling corresponds to a change to a triclinic crystalline structure. Their measurements further show that the two inequivalent Mo chains undergo structural changes essentially independent of one another. Below about 200 K, the distortions in type-1 chains are commensurate with the lattice, whereas the distortion in type-2 chains do not become commensurate until below about 150 K.

In an earlier paper[5] (hereafter referred to as I), we reported the results of a series of nonequilibrium conductivity measurements in Mo_2S_3 below the 145-K phase transition. In these experiments, the sample was heated a few degrees by a large current pulse, and then allowed to rapidly cool while the conductivity was being monitored. After cooling to the initial temperature, the sample conductivity was observed to decrease exponentially with time, with the time constant τ being strongly temperature dependent, according to the equation,

$$\tau=\tau_0\exp(W/kT)\ . \tag{1}$$

The constants τ_0 and W were found to have the values $\sim5\times10^{-15}$ sec and 0.254 eV, respectively. These results suggested that the carriers in Mo_2S_3 could be described phenomenologically in terms of a double-well potential model of the form indicated in Fig. 1. The well on the left-hand side of Fig. 1 corresponds to a relatively highly conducting metastable state for the carriers, while the well on the right-hand side corresponds to a weakly conducting ground state. The presence of the large energy barrier serves to limit the rate of transfer of carriers from one well to the other. The energy difference E was estimated to be on the order of 10–20 meV, or much small-

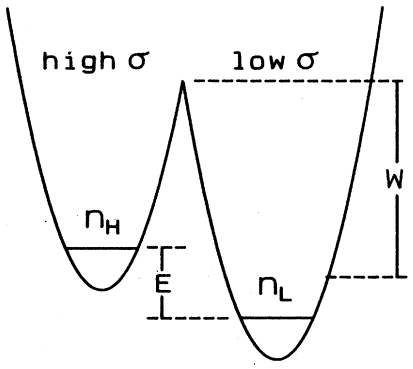

FIG. 1. Double-well potential model for the carriers in Mo_2S_3. The carriers can either be in a low-conductivity ground state (right-hand side) or a relatively high-conductivity metastable state. The energy barrier W between the two states is assumed to be much larger than the energy difference E. n_H and n_L are the equilibrium carrier concentrations in the high- and low-conductivity state, respectively.

er than the barrier height. Assuming that transfer of carriers from one well to the other occurred by thermal activation, this model accurately described the nonequilibrium conductivity measurements.

In this paper, we present the results of measurements of conductivity fluctuations (electrical noise) in Mo_2S_3. It will be seen that the electrical noise has a rather large magnitude as well as strong frequency and temperature dependences. We will show that these measurements are in good agreement with the predictions of the double-well potential model, and further that they require either a very large carrier mobility ($\sim 40\,000$ cm^2/V s) or that on about 10^3 carriers jump from one well to the other simultaneously. This latter possibility would mean that the conductivity in Mo_2S_3 results from a cooperative motion of the carriers, somewhat similar to that observed in charge-density-wave systems. However, no nonlinear conductivity is observed in Mo_2S_3, as it is in the accepted charge-density-wave systems, such as $NbSe_3$ and TaS_3.

In paper I, we suggested three different models for Mo_2S_3 that could give rise to a double-well potential of the form shown in Fig. 1: (1) a defect trapping model; (2) an acoustic polaron (self-trapping) model; and (3) a charge-density-wave model. The measurements presented here are hard to reconcile with models (1) and (2), because they are both independent carrier models that cannot easily give rise to cooperative motion. As will be seen, model (3), while it does naturally result in cooperative motion of the carriers, has other difficulties. If Mo_2S_3 is a charge-density-wave system, it is quite different from the known charge-density-wave systems $NbSe_3$,[10–14] TaS_3,[15–17] $K_{0.3}MoO_3$,[18] and $(NbSe_4)_{3.33}I$.[19]

II. EXPERIMENTS AND RESULTS

The noise measurements were made using a conventional four-probe method (silver-paint contacts), with the samples mounted on a specially designed printed circuit board. The samples and mount were enclosed in a copper can filled with helium exchange gas in order to maintain a uniform temperature. Temperature was measured using a platinum resistance thermometer and was controlled by means of a resistance heater wound around the outside of the copper can.

A. Broadband noise measurements

A schematic diagram of the apparatus used is shown in Fig. 2. A constant current, typically 1–2 mA, was supplied by a battery and a series resistor. The sample voltage was amplified (voltage gain=950) by a homemade preamplifier (after filtering to remove the dc voltage). The noise power level of this amplifier was 2×10^{-18} V^2/Hz for small sample resistances and frequencies above 100 Hz. The noise voltage was further amplified by an Ithaco model 1201 amplifier (typical gain 1000). For the broadband noise measurements, the signal was then sent to an active band-pass filter. The low-pass and high-pass frequencies of this filter was independently adjustable, and the filter slopes were 36 dB/octave. After choosing the low-pass and high-pass frequencies, the amplified noise voltage was measured at equally spaced time intervals using a 12-bit (binary digit) analog-to-digital converter in conjunction with a Digital Equipment Corporation LSI-11 computer. The mean-square voltage fluctuations were calculated and averaged. The computer was also used to read the thermometer and to slowly scan the temperature up or down at a present rate (typically 0.25 K/min). The results of such a measurement on Mo_2S_3 for frequencies between 100 and 3000 Hz (3-dB points) are shown in Fig. 3. The noise power starts increasing at about 220 K. Between 200 and 150 K, the noise power shows rather large fluctuations which are not reproducible in detail. The noise power then goes through a peak near 120 K. Similar curves were obtained for different samples and different frequency ranges. The temperature of the noise maximum depends slightly on the value of the center of the bandpass frequency range.

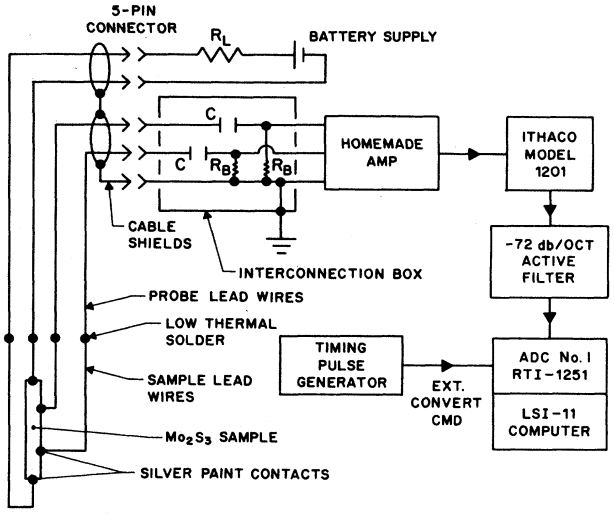

FIG. 2. Schematic diagram of the apparatus used for making broadband electrical noise power measurements.

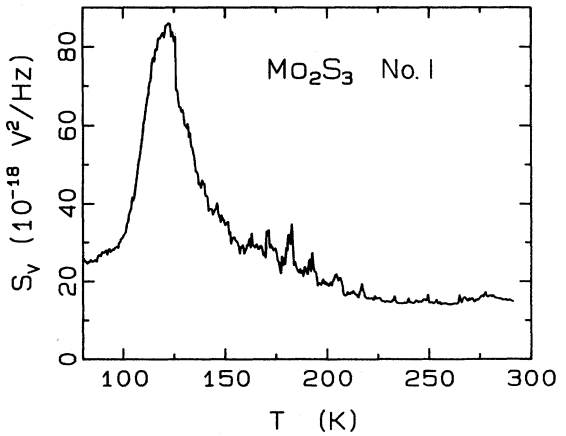

FIG. 3. Broadband noise power of Mo_2S_3 as a function of temperature. The bandpass filter had a low-frequency cutoff of 100 Hz and a high-frequency cutoff of 3000 Hz (3-dB points). This scan was taken on cooling at a rate of 0.25 K/min.

B. Noise amplitude distribution

It is often assumed in noise calculations that the character of the fluctuating observable is such that it is considered to be "stationary" and obeys a Gaussian probability distribution. Then letting $V(t)$ represent an observable which fluctuates with time, then the probability of measuring a value of V between V and $V+dV$ is

$$P(V)dV=\frac{1}{\sqrt{2\pi}}\sigma\exp\left[\frac{-(V-\langle V\rangle)^2}{2\sigma^2}\right]dV\ , \qquad (2)$$

where the quantity $\langle V\rangle$ is the average value of $V(t)$ and σ^2 is its variance, according to $\sigma^2=\langle V^2\rangle-\langle V\rangle^2$.

In order to test the assumption that the electrical noise in Mo_2S_3 was Gaussian, we carried out a measurement of $P(V)$. A constant current was passed through the sample, and the amplified noise voltage was measured at equally spaced time intervals using a 12-bit analog-to-digital (A-D) converter. These data were used to construct a histogram of the number of times a particular value of V occurs versus that value of V. Data were acquired in this manner until 10^4 counts were recorded in any one of the histogram channels.

The histogram was normalized by summing the contents of all channels and dividing the number of counts in each channel by the total. The normalized data then form a histogram representing $P(V)$. The experimental $P(V)$ was then used to calculate the quantities

$$\langle V\rangle=(1/N)\sum_{i=1}^{N}V_iP(V_i)$$

and

$$\sigma^2=(1/N)\sum_{i=1}^{N}(V_i-\langle V\rangle)^2P(V_i)\ ,$$

where N is the total number of histogram channels used (1024). The quantities $\langle V\rangle$, σ^2, and $P(V)$ versus V were then stored on a floppy diskette.

It can be seen that if the $P(V)$ are multiplied by the quantity $(2\pi\sigma^2)^{1/2}$, then the resulting data would represent the function

$$f(V)=\exp(-V^2/2\sigma^2) \qquad (3)$$

if the original data points were sampled from a Gaussian distribution.

Figure 4 shows the results of four voltage amplitude probability measurements which were made at different temperatures on Mo_2S_3 sample 1. The experimental data are shown as dots, and the solid line is, in each case, the function $f(V)$ [Eq. (3)] using the measured variance. For clarity, only one-eighth of the experimental data points have been plotted. The frequency range used in these measurements was from 100 Hz to 3 kHz (3 dB points).

The excellent agreement between the experimental data and Eq. (3) indicates that the fluctuating voltage generated by Mo_2S_3 in the temperature range 77 to 130 K is Gaussian.

C. Measurements of the noise spectra

In order to determine the frequency dependence of the noise power, a series of measurements were made using

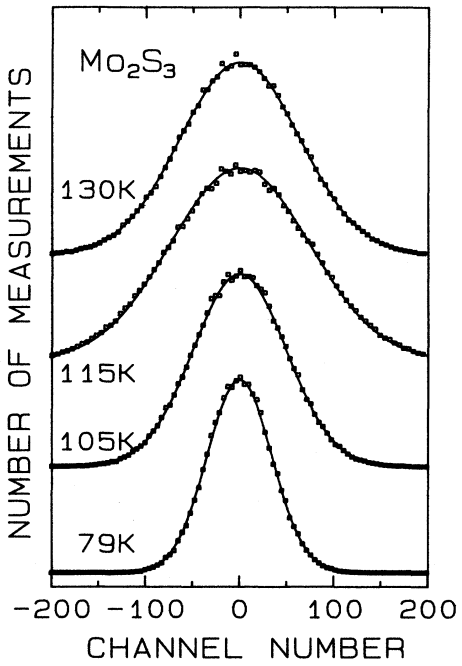

FIG. 4. Voltage amplitude probability measurements in Mo_2S_3. The points show the measured probability amplitudes as a function of channel number (voltage) for four different temperatures. The curves are least-squares-fit Gaussians. Only one data point in eight has been plotted for clarity.

the apparatus of Fig. 2. In this case the band-pass filter of Fig. 2 was replaced by a low-pass filter. The noise voltage was measured at equally spaced time intervals at a rate ranging from 200 to 10 000 voltage readings per second, depending on the frequency range of interest. Typically 1024 voltage readings were recorded and the average value $\langle V\rangle$ was subtracted from the measurements, thus resulting in $\Delta V(t)$, the voltage fluctuations. The Fourier transform of $\Delta V(t)$ was calculated using a fast-Fourier-transform computer subroutine, which gave the coefficients a_K and b_K of

$$\Delta V(t)=\sum_{K=1}^{N}[a_K\cos(2\pi f_Kt)+b_K\sin(2\pi f_Kt)]\ .$$

The frequencies, f_K, are determined by the number of voltage readings taken (N) and the rate (R) at which the voltage readings are taken. To avoid aliasing, the low-pass filter cutoff frequency must be chosen so that no significant signal is present for frequencies above $R/2$.

The coefficients a_K and b_K are used to calculate the spectral coefficients C_K according to

$$C_K=a_K^2+b_K^2\ .$$

The sample temperature was controlled to better than 1 mK, and many such data runs were made (100–1000) at each temperature to determine an ensemble average of C_K. The C_K are multiplied by the appropriate constant which takes into account the amplifier gains and bandwidth of the frequency point Δf so that the noise power data

$$S_K=(\Delta V_K)^2/\Delta f \tag{4}$$

can be calculated.

The noise power spectra of several samples at many different temperatures and currents were measured in primarily three frequency ranges. Since noise is also generated by the electronics and extraneous pickup (mostly 60 Hz and its harmonics from power lines), it was sometimes necessary to measure the noise spectra of a sample with and without a current flowing. The zero-current power spectrum was then subtracted from the nonzero-current spectrum to obtain the desired noise power spectrum.

Two typical noise voltage power spectra $[S_V(f)]$ are shown in Fig. 5. The rapid decrease in $S_V(f)$ on the right-hand side of each plot is due to the -72-dB/octave low-pass filter. The scans shown in Fig. 5 were obtained by averaging 1000 individual data runs, and since the sample-generated noise power is several orders of magnitude greater than the amplifier and extraneous noise, no zero-current subtraction was necessary. Note that the character of the noise power spectrum changes markedly with temperature. As the temperature is lowered, the noise power shifts to lower frequencies.

III. PREDICTIONS OF THE DOUBLE-WELL POTENTIAL MODEL

The double-well potential model introduced in paper I for the charge carriers in Mo_2S_3 is illustrated in Fig. 1. The carriers can be either in a low-conductivity ground state (the right-hand well) or a relatively high-conductivity metastable state, with a large energy barrier (0.25 eV) existing between the two states. The carrier energy in the ground state is approximately 10 meV less than when the carrier is in the metastable state. The height of the energy barrier W and the energy difference E determine the transition rates from one level to the other. Since these transitions are expected to be thermally activated, there should exist random fluctuations in the number of charge carriers in the upper, high-conductivity state. Assuming this to be true throughout the bulk of the sample, then, this fluctuating number of charge carriers will result in a fluctuating sample conductivity. If a constant current is passed through the sample, then the conductivity fluctuations will produce voltage fluctuations between two points along the length of the sample, which can be measured experimentally. In this section, we are going to assume that the conductivity of carriers in the ground state is identically zero. In Sec. V, we will relax this assumption to see how ground-state conduction modifies the predictions of the double-well potential model.

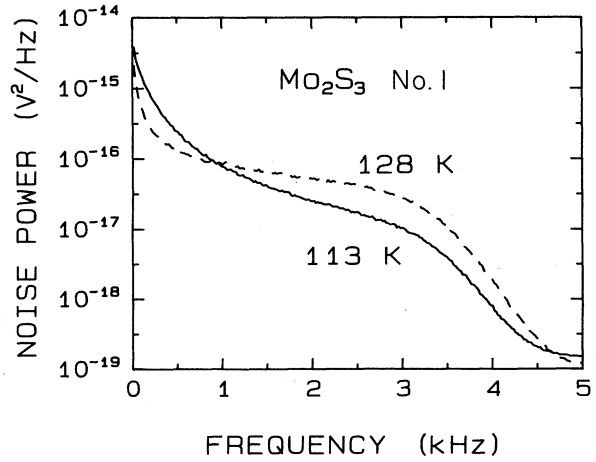

FIG. 5. Noise power spectra of Mo_2S_3 at two different temperatures. The rapid decrease on the right-hand side of each curve is due to the -72-dB/octave filter. Note that as the temperature is lowered, the noise power shifts to lower frequencies.

We write the sample conductivity as

$$\sigma(t)=\frac{e^2\tau_s}{m}n(t)\ ,$$

where n is the free-carrier concentration and τ_s is the carrier scattering time (assumed to be a function of temperature only). Note that τ_s is not in any way related to the carrier relaxation time associated with equilibrium in the double-well potential. The conductivity will fluctuate with the carrier concentration, so that

$$\Delta\sigma(t)=\frac{e^2\tau_S}{m}\Delta n(t)\ .$$

Using Ohm's law $J=\sigma F$, where F is the electric field, and requiring the current to be constant,

$$\Delta J=0=F\,\Delta\sigma(t)+\sigma\,\Delta F(t)\ ,$$

so that

$$\Delta F(t)=-\frac{F(t)}{\sigma(t)}\Delta\sigma(t)=-\frac{F(t)}{n(t)}\Delta n(t)\ .$$

Assuming $\Delta n \ll n$, and using $n=N_H/V_S$, where V_S is the sample volume, and N_H is the total number of carriers in the high-conductivity state, together with $F=V/L$, where L is the sample length and V is the sample voltage, then assuming the conductivity of carriers in the low-conductivity state to be zero, we have,

$$\Delta V(t)=-V\frac{\Delta N_H}{N_H}\ .$$

Thus, the fluctuations in the sample voltage are directly related to the fluctuations in the number of particles in the high-conductivity state. The resulting noise power spectrum can be calculated using any of a number of different approaches. We choose here to calculate the power spectrum using the so-called "single-event" method. Gisolf[20] and Van Der Ziel[21] have used this method to calculate the power spectrum generated by the fluctuating number of free charge carriers in intrinsic semiconductors. In that case, the carriers are thermally generated in pairs (an electron in the conduction band and a hole in the valence band), which exist for a finite time t_r before recombining. During the time in which they are free to contribute to the conductivity, a current pulse is produced in an external circuit. This physical picture is obviously quite similar to the behavior of car-

riers in the double-well potential. The lifetimes of the current pulses are assumed to follow a Poisson distribution, so that the distribution function $g(t)$ can be written as

$$g(t_r)dt_r = \exp(-t_r/\tau)dt_r ,$$

where τ is the average value of t_r. Van der Ziel[21] shows that this gives rise to the power spectrum

$$S_V(f) = \frac{4\langle(\Delta V)^2\rangle\tau}{1+(2\pi f\tau)^2}$$

from which the power spectrum of the sample voltage fluctuations is then easily seen to be

$$S_V(f) = 4\langle V\rangle^2 \frac{\langle \Delta N_H^2\rangle}{\langle N_H\rangle^2} \frac{\tau}{1+(2\pi f\tau)^2} , \quad (5)$$

where $\tau = \tau_0(T)\exp(W/kT)$, and the temperature-dependent prefactor τ_0 is given by (see paper I)

$$\tau_0(T) = \frac{\tau_0}{\exp(E/kT)+\exp(-E/kT)} . \quad (6)$$

The quantities $\langle \Delta N_H^2\rangle$ and $\langle N_H\rangle^2$ can be calculated from statistical-mechanical considerations. If the individual carriers are assumed to be only weakly interacting and the energy of the lower (ground) state is $E_L = 0$, while the energy of the upper (metastable) state is $E_H = E$, then the partition function for N_0 particles distributed between the two levels is

$$Z = [1+\exp(-\beta E)]^{N_0} \quad \text{where } \beta = 1/kT .$$

The average energy of the ensemble is

$$\langle E\rangle = -\frac{\partial(\ln Z)}{\partial\beta} = \frac{EN_0}{1+\exp(\beta E)} .$$

But since $\langle E\rangle = \langle N_H\rangle E$, then this leads to

$$\langle N_H\rangle = N_0/[1+\exp(E/kT)] .$$

It can be shown[22] that for a weakly interacting collection of Maxwell-Boltzmann particles

$$\langle \Delta N_H^2\rangle = -\frac{1}{\beta}\frac{\partial\langle N_H\rangle}{\partial E} .$$

Using the expression for $\langle N_H\rangle$ in this equation and calculating $\langle \Delta N_H^2\rangle$ gives

$$\langle \Delta N_H^2\rangle = \frac{N_0\exp(E/kT)}{[1+\exp(E/kT)]^2} .$$

Substituting these expressions for $\langle N_H\rangle$ and $\langle \Delta N_H^2\rangle$ into Eq. (5) gives the noise voltage power spectrum,

$$S_V(f,T) = \frac{4\langle V\rangle^2\exp(E/kT)}{N_0} \frac{\tau}{1+(2\pi f\tau)^2} , \quad (7)$$

where τ is implicitly a function of temperature.

The reduced noise power $\phi(f,T)$ can be defined as

$$\phi(f,T) = \frac{S_V(f,T)}{\langle V\rangle^2} = \frac{4\tau\exp(E/kT)}{N_0[1+(2\pi f\tau)^2]} . \quad (8)$$

IV. COMPARISON WITH EXPERIMENT

A. Noise power as a function of temperature

Noise power spectra, such as those shown in Fig. 5, were obtained for many temperatures in the range $77 < T < 300$ K, and from these data the noise powers for specific frequencies were determined. This was accomplished by averaging the spectra over a small bandwidth about the desired frequency. Some representative data are shown in Fig. 6, where the reduced noise power for Mo_2S_3 sample 2 is plotted versus temperature for three different fixed frequencies. The noise power is zero for sample temperatures greater than about 200 K, and therefore, these data are shown only for $77 < T < 180$ K.

The solid line in each plot in Fig. 6 is the reduced noise power versus temperature calculated from Eq. (8) using the temperature-dependent relaxation time τ found from the nonequilibrium conductivity measurements on the same sample, assuming $2\pi f = 1/\tau$ at the noise power maximum. (For this sample, we found $\tau_0 = 3\times10^{-15}$ s and $W = 0.254$ eV.) In each case, the agreement between the calculated curve and the experimental data is quite reasonable for temperatures below that of the noise peak, while the agreement is very poor for temperatures larger than this. The high-temperature disagreement becomes progressively worse as the measurement frequency decreases below 3 KHz. Two possible explanations for the disagreement are (1) the superposition of a noise power

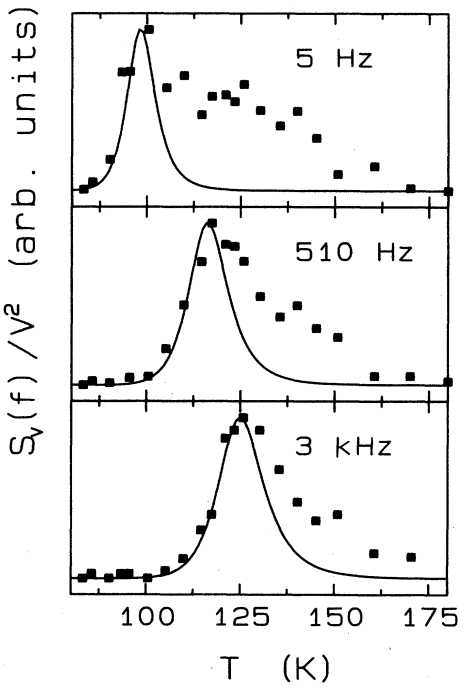

FIG. 6. Narrow-band reduced noise power in Mo_2S_3 as a function of temperature for three different frequencies. The points are the measured reduced noise powers, while the full lines were calculated using Eq. (8) with $\tau_0 = 3\times10^{-15}$ s and $W = 0.254$ eV. These data were obtained on cooling from room temperature at a rate of 0.25 K/min.

spectrum [perhaps of the "$(1/f)$-noise" type] from some, as of yet, unknown source, and/or (2) the dynamics of the phase transition at 145 K, which results in the large hysteresis loop found in the resistivity versus temperature measurements above 125 K. Neither explanation appears satisfactory, because in case (1), the extra noise seems to disappear at the lowest sample temperatures measured at all frequencies, and in case (2), the extra noise is found below 125 K in the 5-Hz plot.

The agreement between the measured data and the calculated curves for temperatures below the noise peak is encouraging, however, and seems to indicate that, at least, a major contribution to the total measured noise power originates from the carrier fluctuations between the wells of the double-well potential.

B. Noise power versus frequency

The partial success of the double-well potential model, noted in Sec. IV A, prompted a more detailed analysis of the frequency dependence of the noise power spectrum. Our raw noise power data, as shown in Fig. 5, shows a dramatic rise in the low-frequency region. In view of this, we assume that a $(1/f)$-noise power contribution[23] to the total measured noise is superimposed on the noise power spectrum given by the double-well potential, according to

$$S_V(f)=\frac{A}{f}+\frac{B\tau}{1+(2\pi f\tau)^2} ,$$

where A and B are (temperature-dependent) parameters which represent the magnitude of each noise contribution, and $S_V(f)$ is the total measured noise power. Multiplying each side of the expression above by f gives

$$fS_V(f)=A+B\frac{\tau f}{1+4\pi^2(\tau f)^2} . \quad (9)$$

The $(1/f)$-noise contribution is seen only as an additive constant in this equation, which is useful, as both f and $S_V(f)$ are experimentally determined quantities.

In order to compare Eq. (9) to experiment, noise power spectra were measured at many sample temperatures in the range $100<T<130$ K. The zero-current noise powers were subtracted (if necessary) and the noise power at each frequency was multiplied by the frequency. Equation (9) was then fit to these values using a nonlinear least-squares fit computer program, which resulted in values of A, B, and τ for each temperature. The measured values of $fS_V(f)$ (dots), and those calculated from the fit to Eq. (9) (solid lines), for six sets of spectral measurements are shown in Fig. 7 for Mo_2S_3 sample 1.

The data in Fig. 7 are in excellent agreement with the calculated curves, especially considering the assumption of a superimposed $(1/f)$-noise term. For systems on which $(1/f)$-noise measurements have been made, the noise power typically varies as $1/f^{\alpha}$, with α approximately, but not exactly equal to 1. α typically falls in the range $0.8<\alpha<1.2$.[23–26] It is possible that even better agreement between Eq. (9) and the measured data could be obtained by allowing α to become a fitted parameter. However, this was not considered necessary in light of the already good agreement using $\alpha=1$. The values of A, B, and τ found in the fits to sample 3 are shown in Table I. As can be seen, the magnitude of B is approximately 30 times the magnitude of A, indicating that noise from the carriers in the double-well potential dominates the $1/f$ noise over most of the frequency range of interest. While τ varies strongly with temperature, A and B are only weakly temperature dependent. Measurements on seven different samples show that for a given sample, the value of A seems to fluctuate randomly about its average value by about $\pm 50\%$ as the temperature is raised from 100 to 130 K. The value of B shows fluctuations of a similar size, but it seems to decrease as the temperature is increased. The temperature dependence of B will be discussed in Sec. IV C.

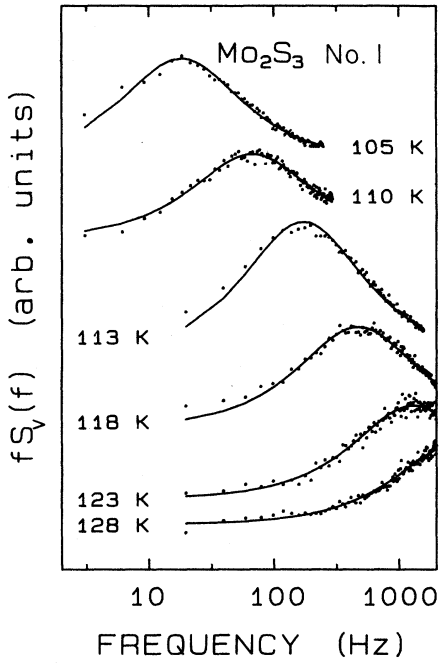

FIG. 7. $fS_V(f)$ as a function of frequency for Mo_2S_3 at several different temperatures. The points are the measured values of $fS_V(f)$, while the full curves were obtained by fitting Eq. (9) to the data.

This method of analyzing the noise power also provides an independent measurement of τ, as compared to that of the nonequilibrium conductivity measurements

TABLE I. Values of A, B, and τ obtained by fitting Eq. (9) to the noise power data on Mo_2S_3 sample 1.

T (K)	A	B	τ (ms)
105.0	34	1380	8.77
109.6	64	1020	2.38
113.4	28	1820	0.929
118.2	31	1080	0.339
123.0	50	840	0.122
127.8	47	720	0.056

discussed in paper I. It is also fortuitous that the noise measurements for τ become useful in the temperature range $100 < T < 130$ K, which is inaccessible to the pulse-conductivity measurements. (For temperatures between 100 and 130 K, the thermal time constants of our sample are longer than the relaxation time associated with the double-well potential.) Plots of $\log_{10}(\tau)$ versus $1/T$ for two different Mo_2S_3 samples are shown in Fig. 8. The squares are the measured values of τ, with the solid squares being obtained from the noise power measurements, and the open squares being obtained from the nonequilibrium conductivity measurements, as discussed in paper I. The solid lines in each case are least-squares fits to the equation $\tau = \tau_0 \exp(W/kT)$. Note that the two values of W agree exactly, and that the two values of τ_0 differ slightly. Also notice that for each sample, the same straight-line fits both the nonequilibrium conductivity measurements and the noise power measurements.

C. Noise power magnitude

The noise power "strength" parameter, B of Sec. IV B, can, by comparison with Eq. (8), be shown to be

$$B = \frac{4V^2}{N_0} \exp(E/kT) , \tag{10}$$

where V is the dc voltage drop between the sample voltage contacts, N_0 is the total number of charge carriers (in both potential wells), and E is the energy difference between carriers in the two potential wells. Since B and T are also measured, a plot of $\ln(4V^2/B)$ versus $1/T$ should, in principle, have a slope $-E/k$, and an intercept $\ln(N_0)$. These data are plotted in Fig. 9 for two different Mo_2S_3 samples. The squares are the measured values, and the lines are least-squares fits. The fitted curves lead to the values $E = 12.5$ meV, $N_0 = 2.6 \times 10^{11}$ for sample 3, and $E = 6.4$ meV, $N_0 = 9.6 \times 10^9$ for sample 1. It is obvious from the figure that there is a considerable scatter in the data, reducing reliability of these values of E and N_0. However, the values of E obtained here are roughly consistent with the estimate $10 < E < 20$ meV made in paper I by looking at the resistivity data. Further, the values of N_0 give the carrier densities 3.3×10^{23} m^{-3} (sample 1) and 1.9×10^{23} m^{-3} sample—within a factor of 2 of each other (the sample volumes differed by a factor of about 16).

An analysis of the noise magnitudes from seven different Mo_2S_3 samples at various frequencies and temperatures gives an average carrier density of $N_0 = (3 \pm 2) \times 10^{23}$ m^{-3}—assuming that the noise is produced by the double-well potential mechanism. All samples show the same carrier densities within our rather large experimental uncertainty. It is important to note that these carrier densities are three orders of magnitude less than the carrier densities estimated from Hall effect measurements. This point will be addressed in Sec. V.

D. Noise power as a function of sample dimensions

Another test for the applicability of the noise power results given by the double-well potential model is the mea-

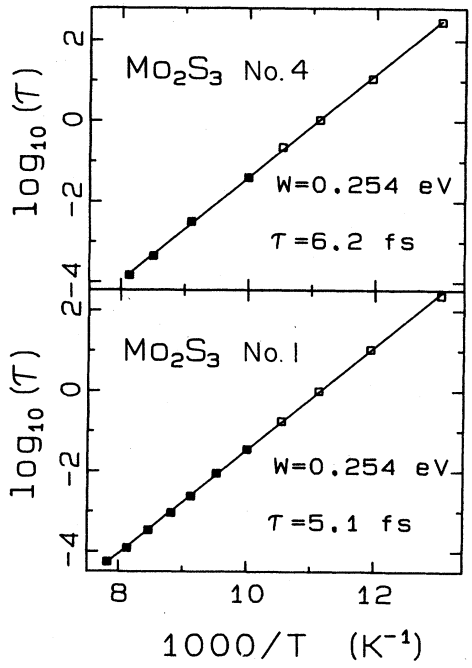

FIG. 8. $\log_{10}(\tau)$ vs $1/T$ for two different samples of Mo_2S_3. The squares are the measured values of τ, with the solid squares being obtained from the noise power measurements and the open squares being obtained from the pulsed conductivity measurements described in paper I. The full lines are least-squares fits to Eq. (1).

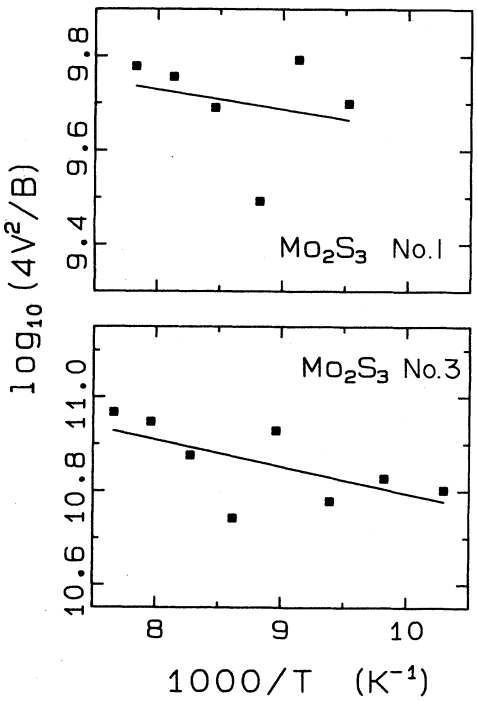

FIG. 9. $\log_{10}(4V^2/B)$ vs $1/T$ for two different Mo_2S_3 samples. The squares are the measured values of $\log_{10}(4V^2/B)$ while the full curves are straight-line fits.

surement of noise power versus sample volume. According to Eq. (8), $\phi \propto N_0^{-1}$, and, assuming $N_0 \propto V_S$, where V_S is the sample volume, then ϕ should be inversely proportional to the sample volume. The data obtained from seven Mo_2S_3 samples, with different volumes, were used to calculate ϕ versus V_S^{-1} for three sample temperatures. These results are shown in Fig. 10. The sample volumes were indirectly measured, due to the small sample dimensions perpendicular to the b axis, using the value of the resistivity ($\sim 1.7\times10^{-3}$ Ω cm at 300 K), and the sample length, measured with a traveling microscope.

It can be seen from the plots, that there is a large scatter in the data, and that only a general trend can be identified—smaller sample volumes tend to generate larger noise signals. However, the data do not provide conclusive evidence supporting the prediction, $\phi \propto V_S^{-1}$. In fact, a plot of ϕ versus A_S^{-1}, where A_S is the estimated sample surface area, shown as Fig. 11, shows that this noise could conceivably be surface generated (which could account for the rather low, noise-determined, carrier density of $n_0 \sim 10^{23}$ m^{-3}). The hypothesis of the noise being generated by a surface effect does not appear to be consistent with the nonequilibrium conductivity results or with the nonequilibrium thermoelectric power results reported in paper I, both of which strongly indicate a bulk effect. If only carriers at the surface were being trapped in the double-well potential ground state, then it seems unlikely that the density of surface states could be large enough to cause the changes observed in the conductivity. A more convincing argument against the surface effect comes from the study of surface states in semiconductors, where a distribution of trap depths is found, leading to a distribution of carrier lifetimes. These surface states are thought to be at least partially responsible for $1/f$ noise in semiconductors (which requires a distribution of relaxation times).[24] However, in Mo_2S_3, a single well-defined time constant is found in both the nonequilibrium conductivity and noise measurements. It is possible that the $1/f$ noise that is found in this compound is due to a surface modification of the bulk state, but it seems doubtful that the surface can be the primary source of the observed carrier lifetimes.

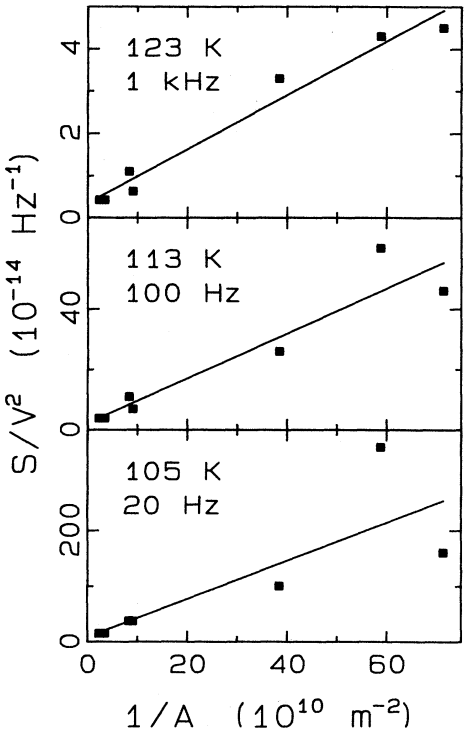

FIG. 11. Noise power magnitude vs sample surface area at three different noise frequencies.

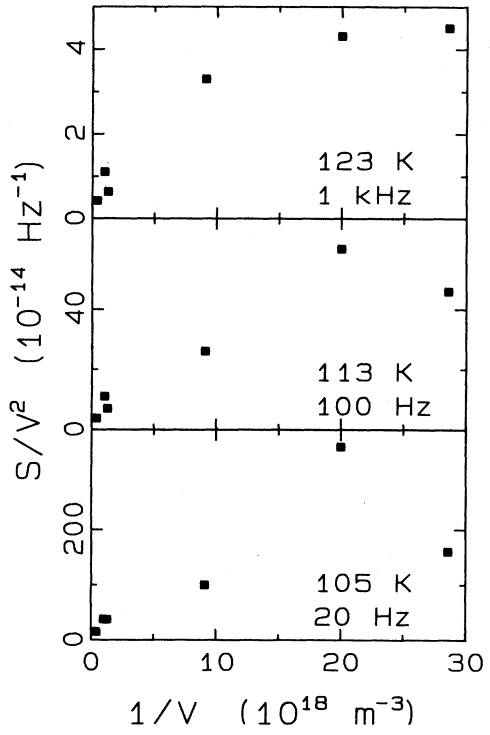

FIG. 10. Noise power magnitude vs sample volume at three different noise frequencies.

It should be pointed out, in connection with the above discussion of surface versus bulk effects, that accurate sample volume measurements are difficult on quasi-one-dimensional compounds. This is particularly true in cases where the sample contact dimensions are roughly the same, or larger, than the sample dimensions between contacts—which is the case for the smallest sample volumes used in the data of Figs. 10 and 11. The volumes calculated for the data in these plots are the "smallest possible" volumes, which were calculated using the wholly unpainted region of the sample between voltage contacts. Since the contacts are approximately of the same length, a maximum possible volume could be as much as a factor of two larger than the minimum volume in some cases. This would provide, generally, a correction in the right direction for the data of Fig. 10, assuming that the noise is, indeed, proportional to the sample volume.

E. Noise power as a function of sample current

A final test made on the noise power magnitude was performed by observing the dependence of noise power on the sample current, I. According to Eq. (8), this dependence should be $S_V \propto I^2$. A plot of S_V versus I^2 is shown in Fig. 12 for a fixed sample temperature and measurement frequency of 125 K and 2 kHz, respectively. As can be seen from these data, $S_V \propto I^2$. (It should be pointed out, however, that it is difficult to find a noise mechanism which does not predict $S_V \propto I^2$.)

V. MODIFICATIONS OF THE DOUBLE-WELL POTENTIAL MODEL

The double-well potential model predicts most of the observed features of the conductivity fluctuations. However, in the development of this model, two assumptions were made regarding the carriers in Mo_2S_3. First, we assumed that all of the carriers in Mo_2S_3 are associated with the double-well potential, with no other kinds of carriers present. Second, we assumed that the carriers in the lower well of the potential do not contribute to the conductivity. Either one, or both, of these assumptions may be wrong, and we now attempt to determine their effect on the predictions of the double-well potential model. As will be seen, relaxing either of these assumptions modifies the double-well potential predictions in much the same way. In what follows, we will first consider the possibility that there are significant numbers of excess carriers in Mo_2S_3 that are not associated with the double-well potential. We will then consider the case where the carriers in the lower well have a nonzero conductivity. In both of these cases we are led to the same conclusions: The energy difference (E) between the ground and metastable conduction states of the double-well potential model is about 26 meV rather than ~ 10 meV, and our estimates of N_0 from the noise measurements are too small by a factor of ~ 2.2.

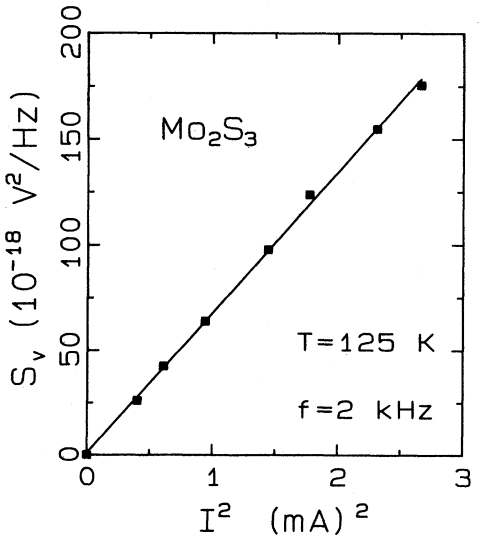

FIG. 12. Noise power at a frequency of 2 kHz vs current squared for Mo_2S_3 at a temperature of 125 K.

A. Excess electron conductivity

There is some justification for assuming that carriers other than those associated with the double-well potential are important in Mo_2S_3. Rastogi and Ray,[2] in their discussion of the transport properties of $Mo_{2.06}S_3$, concluded that their samples contained a considerable number of electrons donated by the excess Mo. They estimated that the electron-to-hole concentration ratio was approximately 5 at 200 K, with the p-type Hall coefficient and thermoelectric power arising from a much greater hole mobility. In addition, the conductivity and Hall-effect behavior above room temperature suggests that electrons are being excited to a low-lying conduction band. While we have little information about the stoichiometry of our samples, we have carried out a simple analysis that sheds some light on this matter.

Let us assume that the conductivity below the lower-temperature phase transition has contributions both from holes (those carriers associated with the *metastable* state of the double-well potential) and from electrons (either due to excess Mo or due to overlapping valence and conduction bands). Then the conductivity can be written

$$\sigma = \sigma_e + \sigma_h \ ,$$

where σ_e is the electron conductivity and σ_h is the hole conductivity. We assume that both the electron and hole scattering times vary inversely with the temperature, and further that the electron concentration is temperature independent, while the hole concentration varies with T as predicted by the double-well potential model. Then we can write

$$\sigma = \frac{K_e}{T} + \frac{K_h}{T[1+\exp(E/kT)]} \ , \tag{11}$$

where K_e and K_h are constants reflecting the relative magnitudes of σ_e and σ_h, respectively.

We have fit Eq. (11) to our conductivity data in the temperature range 85 to 160 K, treating E and K_h/K_e as parameters. The fit cannot be extended to temperatures below about 85 K because the carriers associated with the double-well potential are not in thermal equilibrium, and it cannot be extended above 160 K (on warming) because of the presence of the phase transition. One such fit is shown in Fig. 13. As can be seen, the agreement between experiment and Eq. (11) is quite good (it should be noted that only $\frac{1}{5}$ of the experimental points are shown for clarity). The values of the fitted parameters were $K_h/K_e = 36$ and $E = 25.4$ meV. Similar fits on other scans and other samples lead to values of K_h/K_e ranging from 26 to 53 and to values of E between 25.3 and 26.4 meV, as shown in Table II. These values of K_h/K_e indicate that the hole and electron conductivities are about the same (within a factor of 2) at 80 K, and that the hole conductivity is a factor of 5–10 greater than the electron conductivity at 160 K. It should be noted that the values of E obtained from these fits are a factor of ~ 3 greater than was estimated in Sec. II.

The good fit obtained in Fig. 13 suggests that our samples may indeed have excess electrons in addition to the holes associated with the double-well potential. The ex-

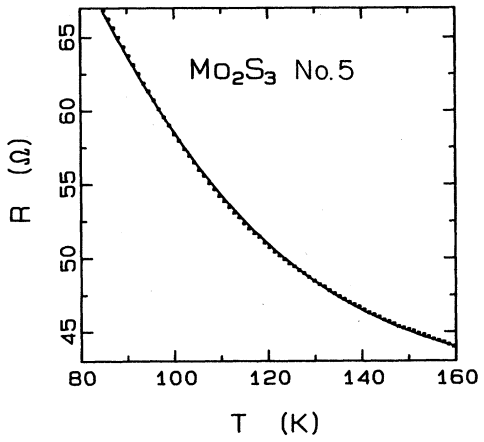

FIG. 13. Electrical resistance of Mo_2S_3 as a function of temperature (on warming). The solid curve is the measured resistance and the dashed curve is a least-squares fit to Eq. (11). Only $\frac{1}{5}$ of the experimental data points are shown for clarity.

cess electrons would presumably also effect the magnitude of the electrical noise, and hence our estimate of N_0. This effect can be estimated in a straightforward fashion. The current density in the sample can be written as

$$J=(\sigma_h+\sigma_e)F ,$$

so that

$$\Delta J=(\sigma_h+\sigma_e)\Delta F+F\,\Delta\sigma_h .$$

Here, only fluctuations in the hole conductivity have been assumed. This is equivalent to assuming that number fluctuations in the double-well potential are much greater than conductivity fluctuations due to random electron scattering processes. Random electron scattering would in any case give rise to a white-noise spectrum—a constant noise background in our measurements.

With this assumption in mind, we require constant current, so that $\Delta J=0$, and thus the fluctuation in sample voltage V can be written as

$$\Delta V=-\frac{V\,\Delta\sigma_h}{\sigma_h+\sigma_e}=-\frac{V\,\Delta\sigma_h}{\sigma_h(1+\sigma_e/\sigma_h)} .$$

Carrying this through the analysis leading to Eq. (7), we obtain the noise power spectrum:

$$S_V(f)=\frac{4V^2\exp(-E/kT)}{N_0(1+\sigma_e/\sigma_h)^2}\frac{\tau}{1+2(\pi f\tau)^2} \tag{12}$$

TABLE II. Values of E and K_h/K_e obtained by fitting Eq. (11) to the temperature-dependent conductivity of Mo_2S_3 in Fig. 13.

W (meV)	K_h/K_e
26.4	52.9
25.3	35.9
25.4	36.6
26.0	25.6

so that Eq. (7) has been simply modified by the factor $(1+\sigma_e/\sigma_h)^2$ in the denominator. This additional factor does not change the frequency dependence of the noise power; it only reduces the magnitude by a few percent. The change in magnitude is important because it is temperature dependent, which means that it will influence the estimates of N_0 and E as obtained from the analysis associated with Fig. 9.

B. Conduction by carriers in the double-well ground state

As a second possibility, we assume that the conductivity of the carriers in the lower well of the double-well potential is not zero. In this case, the total conductivity can be written as the sum of the ground-state conductivity (L) and the metastable state conductivity (H). Assuming once again that carriers in each of the wells have scattering times inversely proportional to T, we have

$$\sigma=\sigma_L+\sigma_H$$
$$=\frac{K_LN_L}{T}+\frac{K_HN_H}{T}$$
$$=\frac{K_LN_0}{T[1+\exp(-E/kT)]}+\frac{K_HN_0}{T[1+\exp(E/kT)]} ,$$

where σ_L and σ_H are the conductivities of the carriers in the lower and higher potential wells, respectively, K_L and K_H are (temperature-independent) constants reflecting the relative magnitudes of the two conductivities, and N_L and N_H are the instantaneous numbers of carriers in the two states. This expression can then be fitted to the experimental conductivity in the temperature range 85–160 K. Such fits to experiment yield values of E which are virtually identical with those obtained assuming excess electrons. The values of K_H/K_L so obtained are all 1.0 greater than the values of K_h/K_e obtained assuming excess electrons. These results are not surprising in view of the rather weak temperature dependence of the $1+\exp(-E/kT)$ factor in the ground state conductivity. Thus we see that both model calculations result in $E\sim 26$ meV.

We can now calculate the noise power in this model. Requiring the fluctuation in current density to be zero gives,

$$T\,\Delta J=(K_LN_L+K_HN_H)\Delta F+F(K_L\Delta N_L+K_H\Delta N_H)=0 .$$

But $N_H+N_L=N_0$, so $\Delta N_L=-\Delta N_H$, and thus

$$\Delta F=-F\frac{1-K_L/K_H}{K_LN_L+K_HN_H}\frac{\Delta N_H}{N_H} .$$

Carrying this through the discussion leading to Eq. (7) results in the modified noise power equation,

$$S_V(f)=\frac{4V^2\exp(E/kT)}{N_0}\left[\frac{1-K_L/K_H}{1+\sigma_L/\sigma_H}\right]^2\frac{\tau}{1+(2\pi f\tau)^2} . \tag{13}$$

So, allowing the carriers in the ground state of the double-well potential to conduct modifies the original

noise power equation by the factor in large parentheses. Note that Eq. (13) is very similar to Eq. (12).

We have carried out a numerical study to see how much the values of N_0 and E are changed by the presence of the conductivity factor. For the case of excess electrons, we can calculate the new noise power "strength" parameter [see Eq. (10)] as

$$B' = \frac{4V^2\exp(E/kT)}{N_0(1+\sigma_e/\sigma_h)^2} = \frac{4V^2\exp(E/kT)}{N_0\{1+(K_e/K_h)[1+\exp(E/kT)]\}^2} . \quad (14)$$

We computed the value of B' for several values of K_h/K_e between 20 and 60 over the temperature range 95–130 K (the temperature range over which our noise data were taken). We then plotted $\log_{10}(4V^2/B')$ versus $1/T$ and performed a linear least-squares fit to the curve for each value of K_h/K_e. This procedure gives estimates of N_0 and E *in the same manner* in which they were estimated from the experimental results presented in Fig. 9. The values of N_0 and E obtained from this procedure are listed in Table III. As can be seen, to lower E from 26 to 12 meV requires $K_h/K_e \sim 40$. Further, this value of K_h/K_e results in N_0 being underestimated by a factor of about 2.2. Although this is a significant change, it is one which will not modify our conclusions to any great extent.

At this point, we return to the conductivity associated with the carriers in the double-well potential. Assuming that carriers in both wells can conduct, we find $K_H/K_L = 40$, and take $n_0 = N_0/V$ to be $3\times10^{23}/m^3$. $K_H/K_L = 40$ means that our estimate of n_0 is too small by a factor of 2.2, and so we take the corrected carrier density to be $6.6\times10^{23}/m^3$ at temperatures below the lower-temperature phase transition. These assumptions lead to the conclusion that the conductivity from carriers in the double-well potential metastable state is about equal to the conductivity from the carriers in the ground state at 80 K. At 160 K, the conductivity from the carriers in the metastable state exceeds those of the ground-state carriers by a factor of 6.

We can also calculate the mobility of the carriers. The measured conductivity at 160 K is approximately $6.7\times10^4\ (\Omega\,m)^{-1}$. So we can write

$$\sigma_{tot} = K_H n_0 \left[\frac{1}{40T[1+\exp(-E/kT)]} + \frac{1}{T[1+\exp(E/kT)]} \right] .$$

From this we find the mobility of the carriers in the metastable state at 160 K to be $4.2\times10^4\ cm^2/V\,s$, and the mobility of the carriers in the ground state to be 1000 $cm^2/V\,s$.

TABLE III. Fitted values of N_0 and E for different values of K_H/K_L. To obtain these values, B' was evaluated from Eq. (14), assuming $N_0 = 10^{10}$ and $E = 0.026$ eV. The values of N_0 and E were then obtained by plotting $\log_{10}(4V^2/B')$ versus $1/T$ and fitting to a straight line for each value of K_H/K_L. This procedure mimics the experimental procedure described in the discussion of Fig. 9.

K_H/K_L	N_0	E (meV)
∞	1.0×10^{10}	26.0
60	5.4×10^9	15.3
50	5.0×10^9	13.8
40	4.5×10^9	11.7
30	4.0×10^9	8.7
20	3.4×10^9	4.1

VI. DISCUSSION

The phenomenological double-well potential model described in this paper and in paper I has been shown to quantitatively predict most features of the observed conductivity and electrical noise behavior in Mo_2S_3 below 145 K. In paper I, it was shown that the double-well potential model could predict the pulsed conductivity measurements very well. In this paper, we have seen that it can also predict the frequency dependence and, to a lesser extent, the temperature dependence of the electrical noise data. Furthermore, if the model is modified to include contributions from other kinds of carriers, the agreement with experiment and the degree of self-consistency improves considerably. In view of the results presented here we believe that an accurate phenomenological description of the conduction properties of Mo_2S_3 is as follows.

Below the lower-temperature phase transition, most of the carriers in Mo_2S_3 can be either in a highly conducting metastable state which lies 0.026 eV above a weakly conducting or nonconducting ground state. The carriers must hop over a large (0.280) eV energy barrier to get from one state to the other. In order to obtain good agreement with the temperature dependence of the conductivity, this picture must be modified slightly so that either carriers in the double-well potential ground state can conduct, or that other kinds of carriers (perhaps electrons donated by excess Mo) must be available to conduct. In either of these cases, the carriers associated with the metastable state dominate the conduction at temperatures above 80 K. Further, our best estimate of the carrier density associated with the double-well potential is $n_0 = 6.6\times10^{23}/m^3$, and when in the metastable state these carriers apparently have a mobility in excess of $4\times10^4\ cm^2/V\,s$.

The most pressing unresolved issue is the nature of the physical mechanism responsible for the double-well potential. In paper I, we considered three possible sources of the double-well potential: (1) the single-carrier trapping model, (2) the acoustic polaron model, and (3) the charge-density-wave model.

The single-carrier trapping model has the advantage of simplicity. In this model, we assume that the carriers are either in a conduction band or are trapped by an intrinsic defect (extrinsic defects appear to be ruled out by the arguments presented in paper I). In this picture, the double-well potential would be a potential in real space, with its shape determined by the nature of the defects.

In the acoustic polaron model, the carriers are "self-trapped" by a localized distortion of the surrounding lat-

tice. The basic ideas leading to this picture were originally developed by Holstein,[27,28] Emin,[29,30] Mott and Davis,[31] Toyozawa,[32,33] and Mott and Stoneham.[34] In the acoustic polaron model, the lattice distorts around the carrier, forming a potential well in which the carrier can sit. The depth of this well depends on the size of the distortion, and hence on the elastic constants of the crystal. Toyozawa has shown that this picture leads to an "adiabatic" potential-energy barrier which separates the electron in the trapped state from the conduction band. Mott and Stoneham[34] showed explicitly that the balance between the particle-in-a-box energy of the trapped electron and the lattice distortion energy can lead to a double-well potential of the form shown in Fig. 1. Estimates of the barrier height in this model are at least roughly consistent with our observed barrier height, lending some credence to this picture.

It should be pointed out that a model containing the salient features of both models 1 and 2 above has been applied to the case of the *DX* center in III-V compounds.[35] The *DX* center is a lattice defect with of yet unknown character which is strongly coupled to the lattice vibrations. When the defect captures a carrier, the lattice strongly relaxes around the electron with a subsequent dramatic lowering of the energy and the formation of a trapped state. This capture mechanism has been called extrinsic self trapping.[36,37] The concentration of *DX* centers is observed to be strongly dependent on the donor concentration. This picture of the *DX* center is described in terms of a double-well potential similar to that used here. In the case of *n*-type GaAs, the trapped carrier is captured in a metastable state lying 0.17 eV above the conduction-band minimum (and also above the Fermi energy), with an 0.33-energy barrier around it. In this case, the metastable state is nonconducting, while the untrapped electron is in the conduction band, which is just the opposite of the situation in Mo_2S_3. However, in $Al_xGa_{1-x}As$ as x is increased from zero, the situation reverses by $x=0.22$, with the metastable (trapped) state lying in the energy gap and below the Fermi energy.[38–40] Long relaxation times are observed at low temperatures in persistent photoconductivity experiments and in transient capacitance measurements.[37] The barrier height appears to be similar in size to that observed here, and the value of τ_0 is generally found to be between 10^{-12} and 10^{-10} s, which is consistent with typical lattice vibrational frequencies, but two to four orders of magnitude larger than we observe in Mo_2S_3. The value of $\tau_0 \sim 5\times10^{-15}$ s suggests that the barrier hopping process in Mo_2S_3 is electronic, rather than lattice dynamical.

The difficulty with the above models is that they are single-carrier models. If the carriers in the double-well potential are independent carriers, then their mobility must be on the order of 4×10^4 cm^2/V s when in the metastable conduction state if the magnitude of the electrical noise power is to be consistent with the magnitude of the electrical conductivity. A mobility this high, while possible, is still very large for carriers in a semimetallic transition metal compound.

At first glance, it would seem reasonable to treat Mo_2S_3 as a charge-density-wave system. Its crystal structure contains linear chains of Mo—S subunits, much as do TaS_3 and $NbSe_3$. Furthermore, it undergoes phase transitions to both commensurate and incommensurate structures at low temperatures, which is also common to charge-density-wave systems. And, the charge-density-wave model eliminates the need for large carrier mobilities in explaining the noise, because cooperative motion of the carriers is possible. Referring back to Eq. (7), the magnitude of the noise power varies as N_0^{-1}. This relationship is fundamental, and to first order independent of the details of the model used to derive it. In the charge-density-wave model, we assume that a whole charge-density-wave segment, containing perhaps 10^3 carriers, can break loose and contribute to the conductivity at once. If so, then 6.6×10^{23} particles/m^3 associated with the double-well potential would each consist of 10^3 carriers. The mobility of each charge density wave segment would then only have to be ~ 40 cm^2/V s, a much more reasonable value for a transition-metal compound.

The difficulty in applying the charge-density-wave model to Mo_2S_3 stems primarily from two observations. First, nonlinear conductivity is not observed in Mo_2S_3, even for large pulsed electric fields. Nonlinear conductivity is easily observed in the two most well-studied quasi-one-dimensional charge-density-wave systems $NbSe_3$ and TaS_3. In these systems, the critical electric field for the onset of nonlinear conduction can be as low as a few mV/cm, whereas in Mo_2S_3, it exceeds 10 V/cm, if indeed it is finite. Second, in both $NbSe_3$ and TaS_3, there is no excess electrical noise due to charge-density-wave motion for small applied electric fields. The critical field for the onset of noise is typically comparable with the critical field for the onset of nonlinear conduction. But in Mo_2S_3, the critical field for the onset of excess noise appears to be zero. The magnitude of the electrical noise seems to be proportional to (current)^2 down to the lowest measurable values. These qualitative differences between the behavior of Mo_2S_3 and those of the two well-studied charge-density-wave systems suggest that different physical processes are responsible for their behaviors.

One possible charge-density-wave model which could explain our results on Mo_2S_3 is one in which the charge-density-wave segments are separated by kinks and antikinks. If a kink and antikink meet, they are mutually destroyed and the charge-density wave can conduct. Such a model has been applied to $NbSe_3$ by Richard *et al.*[41] and by Papoular.[42] To explain our results, the double-well potential would have to be associated with the formation of a kink-antikink pair. The lifetime of the kink-antikink pair would be determined by kink diffusion rates, and would be expected to be strongly temperature dependent, as we observe experimentally. However, it seems premature to consider such a model for conduction in Mo_2S_3 in any detail.

ACKNOWLEDGMENTS

We wish to thank J. R. Hardy, R. J. Hardy, S. S. Jaswal, and D. J. Sellmyer for a number of helpful conversations.

*Present address: Diconix, Inc., 3100 Research Road, P.O. Box 3100 Dayton, OH 45420.
[1]R. DeJonge, T. Popma, G. Wiegers, and F. Jellinek, J. Solid State Chem. **2**, 188 (1970).
[2]A. K. Rastogi and R. K. Ray, Bull. Mater. Sci. **3**, 341 (1981).
[3]M. H. Rashid, D. J. Sellmyer, V. Katkanant, and R. D. Kirby, Solid State Commun. **43**, 675 (1982).
[4]A. K. Rastogi, Philos. Mag. B **52**, 909 (1985).
[5]R. L. Fagerquist and R. D. Kirby, Phys. Rev. B **38**, 3973 (1988).
[6]F. Jellinek, Nature (London) **192**, 2065 (1961).
[7]F. Kadjik, R. Huisman, and F. Jellinek, Acta Crystallogr. Sect. B **24**, 1102 (1968).
[8]R. Deblieck, G. A. Wiegers, K. D. Bronsema, D. van Dyck, G. van Tendeloo, J. van Landuyt, and S. Amelinckx, Phys. Status Solidi A **77**, 249 (1983).
[9]Alova and G. Mozurkewich, J. Phys. (Paris) Colloq. **46**, C10-685 (1985).
[10]P. Monceau, N. P. Ong, A. M. Portis, A. Meerschant, and J. Rouxel, Phys. Rev. Lett. **37**, 602 (1976); N. P. Ong and P. Monceau, Phys. Rev. B **16**, 3443 (1977).
[11]R. M. Fleming and C. C. Grimes, Phys. Rev. Lett. **42**, 1423 (1979).
[12]J. Bardeen, Phys. Rev. Lett. **42**, 1498 (1979); J. Bardeen, Phys. Rev. Lett. **45**, 1978 (1980).
[13]J. R. Tucker, J. H. Miller, Jr., K. Seeger, and J. Bardeen, Phys. Rev. B **25**, 2979 (1982).
[14]G. Grüner, Comments Solid State Phys. **10**, 183 (1983).
[15]T. Sambongi, K. Tsutsumi, Y. Shiozaki, M. Yamanoto, K. Yamaya, and Y. Abe, Solid State Commun. **22**, 729 (1977).
[16]A. H. Thompson, A. Zettl, and G. Grüner, Phys. Rev. Lett. **47**, 64 (1981); G. Grüner, A. Zettl, W. G. Clark, and A. H. Thompson, Phys. Rev. B **23**, 6813 (1981).
[17]G. Grüner, Physica **80**, 1 (1983), and references therein.
[18]C. Schlenker, in *Low-Dimensional Conductors and Superconductors,* edited by D. Jerome and L. G. Caron (Plenum, New York, 1987), p. 477.
[19]A. Meerschaut, P. Gressier, L. Guemas, and J. Rouxel, J. Solid State Chem. **51**, 307 (1984).
[20]J. H. Gisolf, Physica **15**, 825 (1949).
[21]A. Van der Ziel, *Noise* (Prentice-Hall, New York, 1954).
[22]F. Reif, *Fundamentals of Statistical and Thermal Physics* (McGraw-Hill, New York, 1965).
[23]See W. H. Press, Comments Astrophys. Space Phys. **7**, 103 (1978), for an overview.
[24]P. Dutta and P. M. Horn, Rev. Mod. Phys. **53**, 497 (1981).
[25]G. N. Bochkov and Y. E. Kuzovlev, Usp. Fiz. Nauk. **141**, 151 (1983) [Sov. Phys.—Usp. **26**, 829 (1983)].
[26]A. Van der Ziel, Adv. Electron. Electron Phys. **49**, 225 (1979).
[27]T. Holstein, Ann. Phys. (N.Y.) **8**, 325 (1959).
[28]T. Holstein (private communication).
[29]D. Emin, Adv. Phys. **22**, 57 (1973).
[30]D. Emin and T. Holstein, Phys. Rev. Lett. **36**, 323 (1976).
[31]N. F. Mott and E. A. Davis, *Electronic Properties of Non-Crystalline Materials* (Clarendon, Oxford, 1979).
[32]Y. Toyozawa, Prog. Theor. Phys. **26**, 29 (1961).
[33]A. Sumi and Y. Toyozawa, J. Phys. Soc. Jpn. **35**, 137 (1973).
[34]N. F. Mott and A. M. Stoneham, J. Phys. C **10**, 3391 (1977).
[35]D. V. Lang, R. A. Logan, and M. Jaros, Phys. Rev. B **19**, 1015 (1979).
[36]Y. Toyozawa, Solid State Electron. **21**, 1313 (1978).
[37]See D. V. Lang, in *Deep Centers in Semiconductors,* edited by S. T. Pantelides (Gordon and Breach, New York, 1986), for a review of the subject.
[38]L. Dmowski, M. Baj, P. Ioannides, and R. Piotrzkowski, Phys. Rev. B **26**, 4495 (1982).
[39]T. N. Theis, P. M. Mooney, and S. L. Wright, Phys. Rev. Lett. **60**, 361 (1988).
[40]H. P. Hjalmarson and T. J. Drummond, Phys. Rev. Lett. **60**, 2410 (1988).
[41]J. Richard, P. Monceau, M. Papoular, and M. Renard, J. Phys. C **15**, 7157 (1982).
[42]M. Papoular, Phys. Rev. B **25**, 7856 (1982).